Surface and Interface Analysis

WILEY

SURFACE and INTERFACE ANALYSIS

NOTES AND INSIGHTS OPEN ACCESS

Insight Notes: Considerations in the XPS Analysis of O1s Spectra for Metal Oxides

A. Graf[1,2] | M. A. Isaacs[2,3] | D. J. Morgan[1,2]

[1]Translational Research Hub, School of Chemistry, Cardiff University, Cardiff, UK | [2]HarwellXPS, Research Complex at Harwell, Rutherford Appleton Labs, Harwell, UK | [3]Department of Chemistry, University College London, London, UK

Correspondence: D. J. Morgan (morgandj3@cardiff.ac.uk)

Received: 11 October 2025 | **Revised:** 25 November 2025 | **Accepted:** 28 November 2025

Keywords: defect | hydroxide | oxygen | vacancy | XPS

ABSTRACT

The oxygen, O1s core level, is diagnostic in the study of metal oxides, revealing the formation of hydroxides, carbonates and other oxygen-containing species in X-ray photoelectron spectroscopy (XPS). This insight paper gives an overview of the complexities that may be overlooked in the analysis of oxygen core-level spectra and aims to give practitioners of the technique a reasoned approach to the assignment of oxygen speciation.

1 | Introduction

The analysis of metal oxides using X-ray photoelectron spectroscopy (XPS) is common, given their role in areas such as catalysis, energy storage, electronics and the understanding of corrosion [1–4]. Understanding changes in the surface chemistry of metal oxides, such as reduction or the formation of hydroxides and carbonates, allows significant mechanistic insight into the surface processes occurring.

Regretfully, it is not uncommon for photoelectron spectra to be both over and erroneously analysed by inexperienced analysts, although efforts are being made to combat this [5, 6]. To date, papers have been published on the analysis of C1s spectra [7, 8]; however, data within this spectral region generally complement the O1s spectrum, and if the analyst is to quantify the oxygen spectrum with confidence, then all sources of oxygen should be accounted for. This has led to the availability of calculators to correct for the oxygen associated with adventitious carbon [9].

In this paper, we introduce for those new to XPS, a logical approach to the analysis of O1s spectra for metal oxides and whilst we will not focus on polymers, we note excellent resources on the binding energies for polymer oxygen functionalities have been previously published [10, 11]. Furthermore, we wish the reader to note the logical approach discussed herein for metal oxides is equally valid for the analysis of polymers and other materials.

2 | Discussion

We split our discussion into smaller, focused sections. Where we present O1s binding energies, these have been calibrated to 284.8 eV and cross-checked using the metal core-line as a secondary reference point [12].

2.1 | Features of the O1s Spectrum

The O1s spectrum of metal oxides will generally have contributions from lattice oxygen (O^{2-}), hydroxide (-OH) and carbonate ($-CO_3$), the proportions of which will depend on the sample storage and handling. As shown in Figure 1, each of these species

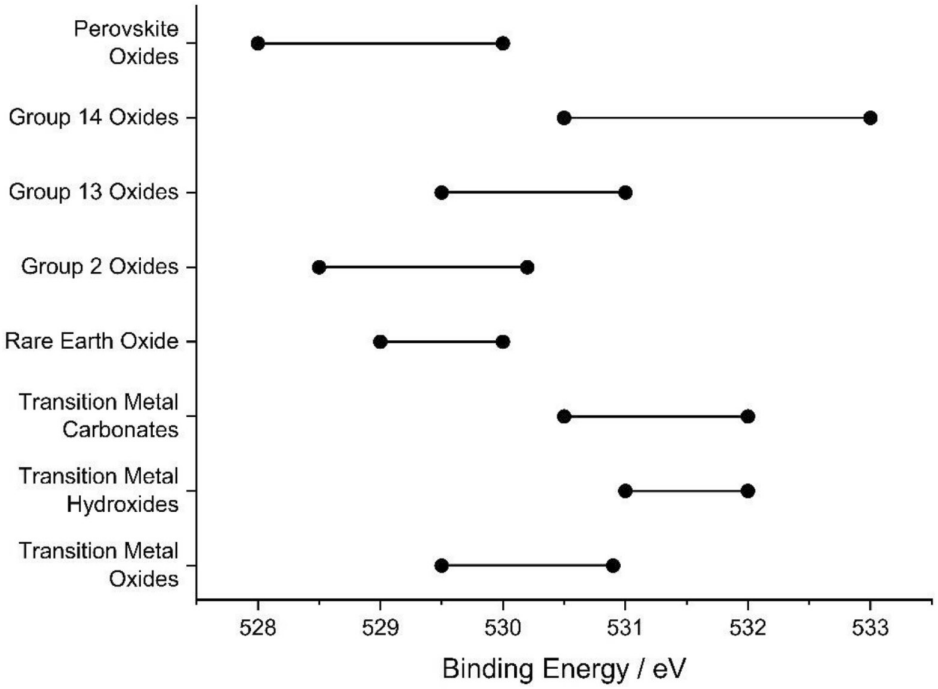

FIGURE 1 | Plot of O1s binding energy ranges collated from [14].

has a distinct binding energy range, which is influenced by the bonding of the metal to the ligand. This bonding is, in turn, affected by the size and coordination of the metal cation [13].

Clearly as Figure 1 shows, there are overlapping energies for oxides and hydroxides, and similar overlaps for hydroxide and carbonates. Subsequently, before assignment of any surface chemistry, possible surface species should be identified based on knowledge of the sample history (such as handling, storage or a reaction environment) and the presence of a corroborating signal, for example, a C1s signal at ~289 eV for carbonate.

Other oxygen signals may arise from sulphates (~168–169.5 eV) [14, 15] and phosphates (~531–533 eV) [16, 17], whilst for Na-containing compounds, signals arising from the Na KLL Auger–Meitner signal when using an aluminium X-ray source can add further confusion.

Small energy loss features may also be noted roughly between 4 and 12 eV above the lattice oxide signal, and their positions measured by reflection electron energy loss spectroscopy (REELS)—see, for example, CeO_2 and TiO_2 [18, 19].

2.2 | Fitting of the O1s Spectrum

Fitting of the O1s spectrum is not always necessary, and a more qualitative view of the spectrum can be taken. Should fitting be required, the minimum number of justifiable peaks should be used to avoid possible over interpretation of the spectral envelope. All data presented has been acquired using a Thermo Scientific K-alpha$^+$ photoelectron spectrometer at pass energies of 40 eV, the 400-μm spot mode, which gives an X-ray power of 72 W (6 mA × 12 kV). The spectra were recorded using a 0.1 eV step size and a 50 ms dwell time and using a dual-beam charge compensation system (Beam 0.4 V, emission 150 μA, focus 20 V, extract 50 V and a gas cell voltage of 20 V). All data has been calibrated to the C1s peak taken to be 284.8 eV.

2.3 | Simple Oxides

Unless a material exhibits a significantly rich and varied surface chemistry, such as that in perovskite oxides [20, 21], then generally two or three peaks are sufficient. Depending on the pass energy and assuming good charge compensation, the FWHM of the peaks will generally be between ~1.2–1.6 eV, with hydroxides, sulphates and phosphates generally slightly higher, varying between ~1.6–2.0 eV.

This can be seen in Figure 2, where the O1s spectra of hydrated MgO and a commercial ZrO_2 are fitted with lattice oxide and hydroxide signals only because the C1s spectra show minimal adventitious carbon contamination. In both cases, the spectra have been fitted with a Voigt-like function (LA(50) in CasaXPS) and reveal FWHM of ~1.4 eV for the lattice oxide and ~2.0 eV for the hydroxide.

The spectra in Figure 2 are simple cases, and whilst it can be argued that fitting is not necessarily required, they do illustrate the need to keep to a minimum number of justifiable peaks for fitting and that not all peaks for a given core-level will have the same FWHM.

2.4 | Complex Oxide Systems

A more complicated example is shown in Figure 3, where the fitted O1s and associated core-level spectra for an air-exposed perovskite, $LaSrCoO_3$, are shown. These materials are known

to react with the atmosphere, forming carbonates [20] and may also undergo some degree of surface segregation [21]. The complex O1s spectral envelope is generally interpreted as different oxides, with molecular oxygen and water [22].

To analyse the O1s spectrum with increased confidence, information from all other core-levels must be considered. From the C1s spectrum (Figure 3d), we note the presence of carbonate at ~289 eV; hence, we should expect some CO_3 contribution to the O1s spectrum (between 530 and 532 eV based on Figure 1).

The Co2p spectrum (Figure 3e) reveals a single, Co_3O_4-like oxide state [23], whereas inspection of the $La3d_{5/2}$ spectrum (Figure 3b) notes that the shape and splitting of the $La3d_{5/2}$ are not commensurate with those of reference La compounds. Subsequent fitting reveals two La states with $3d_{5/2}$ splitting values of 3.8 and 3.4 eV, likely attributable to La–OH (or La–O–OH) and La–CO_3 bonds [24, 25]. Hence, we expect a signal for OH in the O1s spectrum in addition to that already noted for CO_3.

Finally, fitting of the Sr3d spectrum (Figure 3c) reveals three distinct states at ~131.5, 133.5 and 135.0 eV. Whilst there is a

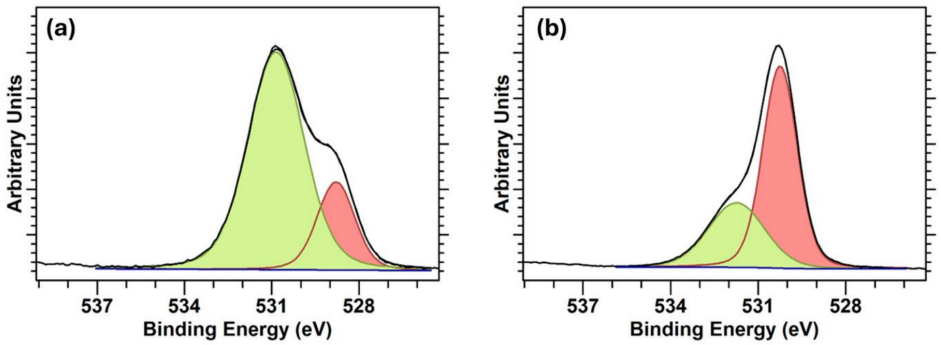

FIGURE 2 | Fitted O1s spectra of (a) hydrated MgO and (b) fresh ZrO_2. Red = lattice oxygen and green = surface hydroxide.

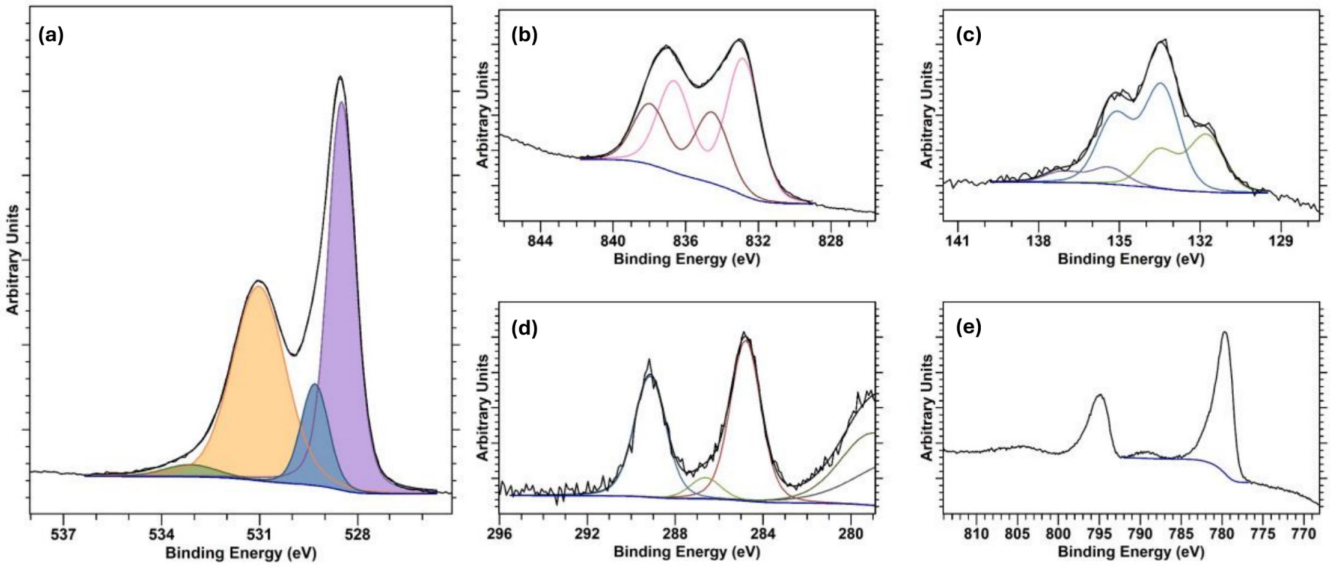

FIGURE 3 | (a) Fitted O1s spectrum for $LaSrCoO_3$, with (b) $La3d_{5/2}$, (c), Sr3d (d) C1s and (e) Co2p core-level spectra showing the different speciation for each element. For clarity, the spin–orbit splitting for the peaks have been merged into individual peak envelopes. The O1s assignments are discussed in the main text and Table 1.

TABLE 1 | Assignments of the O1s species in Figure 3a supported by analysis of the other core-level spectra.

O1s binding energy/eV	Peak FWHM/eV	Assignment	Reference(s)
528.5 (purple)	1.1	Lattice oxygen in perovskite	[26, 27, 29–31]
529.5 (blue)	1.2	M–O (M = Co, Fe, Sr) in oxide	[26, 27, 30, 31]
531.0 (orange)	1.8	Hydroxyl groups and carbonate	[20, 26, 27, 30, 31]
533.0 (green)	1.9	Organic, water or loss feature	[12, 26, 27, 29, 30, 32, 33]

degree of uncertainty in the binding energy of some pure Sr compounds, likely due to surface hydroxides and/or carbonates in previously measured reference materials, these energies are generally attributed to Sr in the perovskite, $Sr(OH)_2/SrCO_3$, and Sr-halides [12]. However, as the sample is halide-free, it is possible these are caused by SrO-like islands, as noted for $SrTiO_3$ and similar materials [26–28].

Armed with knowledge of the metal speciation, we can fit and assign the O1s spectrum, as shown in Figure 3a, with a more informed view. Whilst there may still be some uncertainty due to the multiple possible oxides, hydroxides and carbonates, we can assign the species as shown in Table 1.

The peak assigned as hydroxide at 531 eV is broad and consistent with the larger FWHM expected for these compounds. The peak around 533 eV has previously been attributed to water, although this is typically achieved at cryogenic temperatures [34]. Under vacuum conditions of $<10^{-9}$ mbar, it is likely that water will have desorbed; hence, this is a result of a surface carbonate species or a loss feature inherent to the O1s spectrum. Furthermore, it has been shown that water on $LaCoO_3$ dissociates to form hydroxide and that no molecular water is noted under UHV [35]. More importantly, the assignment of the species is consistent with that predicted from computational modelling with tandem experimental analysis [30].

Any further analysis than the above would be mostly futile but also highlights the need for users to either record their own, traceable reference spectra for comparison or refer to peer-reviewed reference data such as those in [36].

2.5 | Overlapping, Neighbouring and Screened Photoelectron Signals

The successful analysis of the oxygen speciation can be complicated by overlapping signals (e.g., $Sb3d_{5/2}$ and $Pd3p_{3/2}$), neighbouring photopeaks (e.g., $V2p_{1/2}$) or Na KLL Auger–Meitner peaks, as previously stated. In such cases, peak shapes derived from bulk compounds and fitting constraints, such as spin–orbit splitting, can be used, and some examples are shown in Figure 4.

La_2O_3 (Figure 4a) has a lattice oxide peak at 530.5 eV, with a second between 532 and 533 eV, which was previously attributed to water or hydroxide groups [25]. As discussed in [25], the expected stoichiometry is observed, with no evidence in the valence band spectrum for water or hydroxide, and the origin of this peak has been linked to structural effects. Materials such as Sb_2O_3 (Figure 4b) and mixed Pd metal and oxide systems (Figure 4c) can be fitted using known spin–orbit splitting ratios and distances, using information from other primary (e.g., Pd3d) core-levels for evidence of multiple metal speciation.

There are instances where features in the O1s spectrum, such as screened states, can be misinterpreted as a particular state. For example, the O1s spectrum for the anhydrous form of the conducting oxide IrO_2 has an asymmetric profile with an apparent shoulder at ~531 eV. Based on binding energies alone, this could be assigned as hydroxide; however, this has been shown to be a screened state caused by conduction electrons [37, 38], although a higher intensity would suggest hydroxide is present and the sample is becoming hydrated [37].

2.6 | A Comment on Oxygen Vacancies

The role of oxygen vacancies in surface reactivity is well known and therefore cannot be overlooked in the present discussion of O1s spectra. Many papers have discussed oxygen vacancies and the actual assignment to oxygen species in the range 531–532 eV [33, 39–41], whilst a recent paper by one of the present authors critically examines the use of XPS in such analysis [6], consequently, we exhibit brevity in our discussion here.

The basis of XPS requires the ejection of a photoelectron and measuring its kinetic energy to infer a binding energy. The term vacancy implicitly implies there is no electron to eject, so we consequently cannot measure these vacancies. Any vacancy, given its increased reactivity, will quickly become saturated through the dissociative adsorption of gaseous species (e.g., water).

To highlight this common misnomer, we show in Figure 5, the argon cluster etching (6 kV, 2000 atoms, 20 s per cycle) of a TiO_2 single crystal. Evident in the overlayed Ti2p spectra is the formation of reduced Ti^{3+} states; however, the corresponding O1s

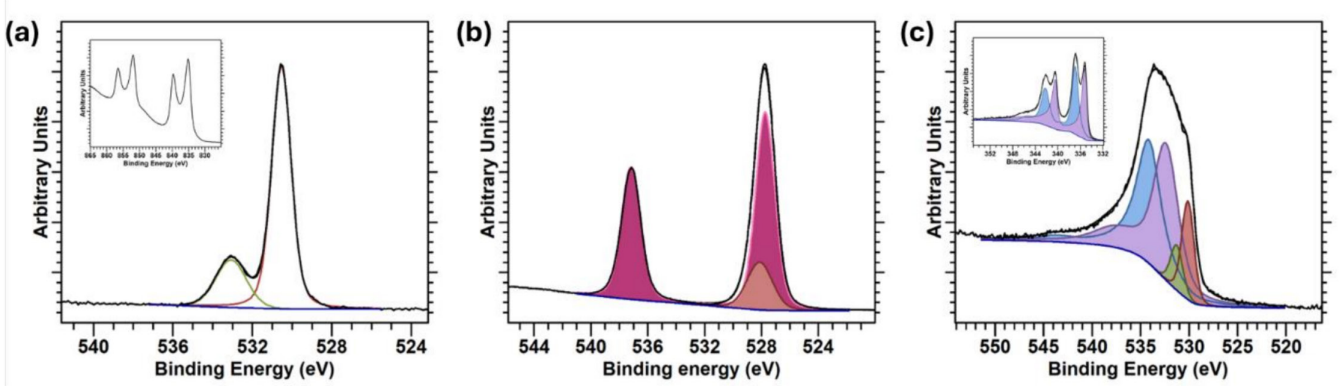

FIGURE 4 | Core-level spectra for (a) La_2O_3, (b) Sb_2O_3 (dark pink = Sb, pink = O) and (c) a mixed, Pd/PdO system (blue = PdO, lilac = Pd metal, green and red are hydroxide and oxide respectively). Inserts, where plotted, show the primary metallic core-levels.

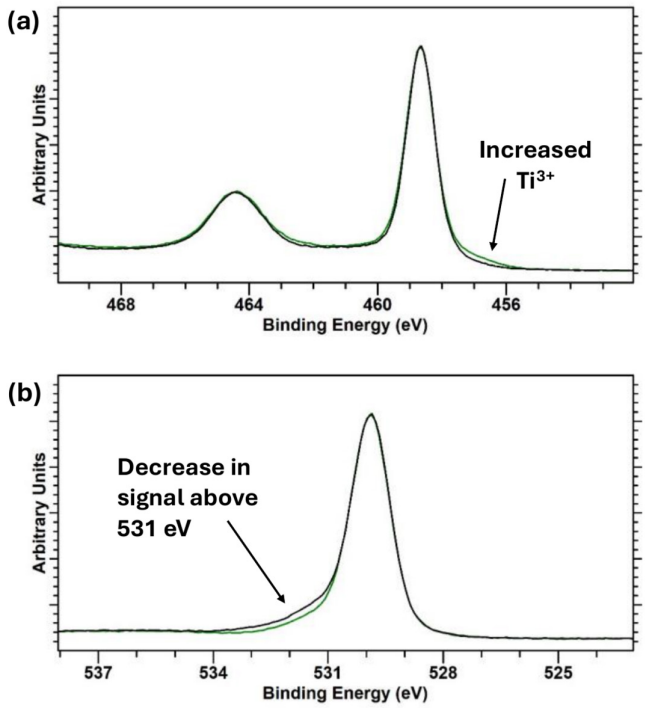

FIGURE 5 | Overlayed (a) Ti2p and (b) O1s spectra of fresh (black) and cluster etched (green) single crystal TiO_2 showing as reduced Ti states form, there is a concomitant decrease in the spectral region typically assigned to vacancies.

spectra reveal a decrease in the high binding energy shoulder, going against the assignment of a vacancy peak.

Such observations are supported by computational modelling which indicates the binding energy of defective lattice oxygen should only differ by ~0.2 eV [41–43] and that the quantification of defects should be made via Raman [44, 45] or inferred from the presence of reduced metallic states, such as Ti^{3+} [46], noting some measurements would be characterising the bulk defect density.

2.7 | Why Does the Lattice Oxide Binding Energy Change?

A question commonly asked by those new to XPS is why the lattice oxide peak differs in binding energy between, for example, SiO_2 and TiO_2.

Recall that the binding energy of a photoelectron will change depending on the nature and strength of the bonding of the emitting atom to another atom, such as a ligand, and the degree of charge transfer. For metal oxides, the degree of covalency (or ionicity) will influence the M–O bond strength; hence, the observed binding energy.

Taking the example of SiO_2 and TiO_2, we note that the Si–O bond (binding energy 532.7 eV) is more covalent than the Ti–O bond (binding energy 529.8 eV) and hence exhibits a higher binding energy. Similarly, for more ionic character in M–O bonds, we note a decrease in the binding energy. These observations can be linked to the oxygen ions in covalent systems being less charged than a corresponding ionic system, where the charge on the oxygen is more localised [47–49]. This is exemplified by comparing CeO_2 and UO_2, where despite identical electronegativity differences and Madelung potentials, partial charge analysis suggests that CeO_2 is more ionic and this is observed in the lattice oxygen binding energies, which differ by ~1 eV [47]. However, there will always be factors causing deviations from this, as discussed by Bagus and co-workers [13, 50–52].

2.8 | Near-Ambient Pressure XPS (NAP-XPS)

In our discussion herein, we cannot ignore the increased availability of near-ambient pressure (NAP) systems, which have opened new avenues in XPS analysis and introduced new oxygen signals to the O1s spectrum.

In these systems, charge compensation is typically achieved using a noble gas or air [53], or water [54]. Each of these gases will have their own gas phase spectroscopic signature [55, 56]. Consequently, in addition to the lattice oxygen of a metal oxide, species that may be present include a thin liquid water layer, oxygen-containing gaseous species (e.g., O_2, NO, CO and CO_2) and other reaction gases [57, 58].

Thankfully, the binding energy of oxygen-containing gas-phase species is generally found at energies greater than 533 eV than surface species, so overlap is minimal; a detailed discussion with examples of such NAP-XPS experiments is given in [58, 59].

3 | Summary

This note has been prepared to address the over analysis of O1s spectra which, like its C1s counterpart, is becoming commonplace in the literature. A simple, systematic approach has been discussed, which utilises metallic, C1s and other core levels to assess the contributions to the O1s spectra. The approach has been highlighted with worked examples of differing complexity.

Although focused on the oxygen spectra, we emphasise the logical approach presented herein applicable to all spectral regions, where cross-referencing with other core levels to elucidate possible chemical states should be made.

Author Contributions

D. J. Morgan: conceptualisation, writing original draft, original data collection, data curation, formal analysis. **M. A. Isaacs:** review and editing of original draft. **A. Graf:** review and editing of original draft.

Funding

Some of the work included herein has been generated through the authors' provision of the EPSRC National Facility for Photoelectron Spectroscopy (HarwellXPS) ('HarwellXPS', EP/Y023587/1, EP/Y023609/1, EP/Y023536/1, EP/Y023552/1 and EP/Y023544/1).

Ethics Statement

The authors have nothing to report.

Conflicts of Interest

The authors declare no conflicts of interest.

Data Availability Statement

Data sharing not applicable to this article as no new datasets were generated or analysed during the current study.

References

1. R. Schlögl, "Heterogeneous Catalysis," *Angewandte Chemie, International Edition* 54, no. 11 (2015): 3465–3520.

2. G. Ertl, H. Knözinger, and J. Weitkamp, *Handbook of Heterogeneous Catalysis* (Wiley-VCH Verlag GmbH & Co., 2008).

3. J. C. Védrine, *Metal Oxides in Heterogeneous Catalysis* (Elsevier, 2018), 1–596.

4. R. Lindsay and A. Thomas, "Introducing X-Ray Photoelectron Spectroscopy for Corrosion Studies: A Tool for Elucidating Interfacial Composition and Chemistry," in *Water-Formed Deposits* (Elsevier, 2022), 723–745.

5. G. H. Major, T. G. Avval, B. Moeini, et al., "Assessment of the Frequency and Nature of Erroneous X-Ray Photoelectron Spectroscopy Analyses in the Scientific Literature," *Journal of Vacuum Science & Technology A* 38, no. 6 (2020): 061204.

6. C. D. Easton and D. J. Morgan, "Critical Examination of the Use of X-Ray Photoelectron Spectroscopy (XPS) O 1s to Characterize Oxygen Vacancies in Catalytic Materials and Beyond," *Journal of Vacuum Science & Technology A* 43, no. 5 (2025): 053205.

7. D. J. Morgan, "Comments on the XPS Analysis of Carbon Materials," *C (Basel)* 7, no. 3 (2021): 51.

8. T. R. Gengenbach, G. H. Major, M. R. Linford, and C. D. Easton, "Practical Guides for X-Ray Photoelectron Spectroscopy (XPS): Interpreting the Carbon 1s Spectrum," *Journal of Vacuum Science & Technology A: Vacuum, Surfaces, and Films* 39, no. 1 (2021): 013204.

9. J. D. Henderson, B. P. Payne, N. S. McIntyre, and M. C. Biesinger, "Enhancing Oxygen Spectra Interpretation by Calculating Oxygen Linked to Adventitious Carbon," *Surface and Interface Analysis* 57, no. 3 (2025): 214–220.

10. G. P. López, D. G. Castner, and B. D. Ratner, "XPS O 1s Binding Energies for Polymers Containing Hydroxyl, Ether, Ketone and Ester Groups," *Surface and Interface Analysis* 17, no. 5 (1991): 267–272.

11. G. Beamson and D. Briggs, *High Resolution XPS of Organic Polymers: The Scienta ESCA300 Database* (Wiley-Blackwell, 1992).

12. D. J. Morgan, "The Utility of Adventitious Carbon for Charge Correction: A Perspective From a Second Multiuser Facility," *Surface and Interface Analysis* 57, no. 1 (2025): 28–35.

13. G. Pacchioni and P. S. Bagus, "Theoretical Analysis of the O(1*s*) Binding-Energy Shifts in Alkaline-Earth Oxides: Chemical or Electrostatic Contributions," *Physical Review B* 50, no. 4 (1994): 2576–2581.

14. NIST X-ray Photoelectron Spectroscopy Database, "NIST Standard Reference Database Number 20, National Institute of Standards and Technology," Gaithersburg MD, 20899 (2000).

15. M. Wahlqvist and A. Shchukarev, "XPS Spectra and Electronic Structure of Group IA Sulfates," *Journal of Electron Spectroscopy and Related Phenomena* 156–158 (2007): 310–314.

16. V. Bemmer, M. Bowker, J. H. Carter, et al., "Rationalization of the X-Ray Photoelectron Spectroscopy of Aluminium Phosphates Synthesized From Different Precursors," *RSC Advances* 10, no. 14 (2020): 8444–8452.

17. P. M. A. Sherwood, "Introduction to Studies of Phosphorus-Oxygen Compounds by XPS," *Surface Science Spectra* 9, no. 1 (2002): 62–66.

18. C. Baeumer, A. Y.-L. Liang, U. Trstenjak, et al., "Carbonate Formation Lowers the Electrocatalytic Activity of Perovskite Oxides for Water Electrolysis," *Journal of Materials Chemistry A* 9, no. 35 (2021): 19940–19948.

19. B. Koo, K. Kim, J. K. Kim, H. Kwon, J. W. Han, and W. Jung, "Sr Segregation in Perovskite Oxides: Why It Happens and How It Exists," *Joule* 2, no. 8 (2018): 1476–1499.

20. H. Liu, Y. Wang, P. Tan, et al., "A Doping-Induced $SrCo_{0.4}Fe_{0.6}O_3$/$CoFe_2O_4$ Nanocomposite for Efficient Oxygen Evolution in Alkaline Media," *Small* 20, no. 21 (2024): 2308948.

21. M. C. Biesinger, B. P. Payne, A. P. Grosvenor, L. W. M. Lau, A. R. Gerson, and R. St. C. Smart "Resolving Surface Chemical States in XPS Analysis of First Row Transition Metals, Oxides and Hydroxides: Cr, Mn, Fe, Co and Ni." *Applied Surface Science* 257, no. 7 (2011): 2717–2730.

22. J. P. H. Li, X. Zhou, Y. Pang, et al., "Understanding of Binding Energy Calibration in XPS of Lanthanum Oxide by In Situ Treatment," *Physical Chemistry Chemical Physics* 21, no. 40 (2019): 22351–22358.

23. M. F. Sunding, K. Hadidi, S. Diplas, O. M. Løvvik, T. E. Norby, and A. E. Gunnæs, "XPS Characterisation of In Situ Treated Lanthanum Oxide and Hydroxide Using Tailored Charge Referencing and Peak Fitting Procedures," *Journal of Electron Spectroscopy and Related Phenomena* 184, no. 7 (2011): 399–409.

24. A. Galenda, M. M. Natile, and A. Glisenti, "$La_{0.6}Sr_{0.4}Co_{0.8}Fe_{0.2}O_{3-\delta}$ and Fe_2O_3/$La_{0.6}Sr_{0.4}Co_{0.8}Fe_{0.2}O_{3-\delta}$ Powders: XPS Characterization," *Surface Science Spectra* 13, no. 1 (2006): 31–47.

25. M. M. Natile, F. Poletto, A. Galenda, and A. Glisenti, "$La_{0.6}Sr_{0.4}Fe_{0.6}Co_{0.2}Cu_{0.2}O_{3-\delta}$ Powders by XPS," *Surface Science Spectra* 16, no. 1 (2009): 58–66.

26. B. Psiuk, J. Szade, M. Pilch, and K. Szot, "XPS Studies of Perovskites Surface Instability Caused by Ar+ Ion and Electron Bombardment and Metal Deposition," *Vacuum* 83 (2009): S69–S72.

27. A. Nenning, A. K. Opitz, C. Rameshan, et al., "Ambient Pressure XPS Study of Mixed Conducting Perovskite-Type SOFC Cathode and Anode Materials Under Well-Defined Electrochemical Polarization," *Journal of Physical Chemistry. C, Nanomaterials and Interfaces* 120, no. 3 (2016): 1461–1471.

28. A. Whitten, D. Guo, E. Tezel, R. Denecke, E. Nikolla, and J.-S. McEwen, "Deconvoluting XPS Spectra of La-Containing Perovskites From First-Principles," *JACS Au* 4, no. 8 (2024): 3104–3117.

29. D. A. Pawlak, M. Ito, M. Oku, K. Shimamura, and T. Fukuda, "Interpretation of XPS O (1s) in Mixed Oxides Proved on Mixed Perovskite Crystals," *Journal of Physical Chemistry. B* 106, no. 2 (2002): 504–507.

30. N. A. Merino, B. P. Barbero, P. Eloy, and L. E. Cadús, "$La_{1-x}Ca_xCoO_3$ Perovskite-Type Oxides: Identification of the Surface Oxygen Species by XPS," *Applied Surface Science* 253, no. 3 (2006): 1489–1493.

31. D. J. Morgan, "Photoelectron Spectroscopy of Ceria: Reduction, Quantification and the Myth of the Vacancy Peak in XPS Analysis," *Surface and Interface Analysis* 55, no. 11 (2023): 845–850.

32. M. Henderson, "The Interaction of Water With Solid Surfaces: Fundamental Aspects Revisited," *Surface Science Reports* 46, no. 1–8 (2002): 1–308.

33. M. Oku, H. Matsuta, K. Wagatsuma, Y. Waseda, and S. Kohiki, "Removal of Inelastic Scattering Part From Ti2p XPS Spectrum of TiO_2 by Deconvolution Method Using O1s as Response Function," *Journal of Electron Spectroscopy and Related Phenomena* 105, no. 2–3 (1999): 211–218.

34. M. H. Engelhard, D. R. Baer, A. Herrera-Gomez, and P. M. A. Sherwood, "Introductory Guide to Backgrounds in XPS Spectra and Their Impact on Determining Peak Intensities," *Journal of Vacuum Science & Technology A* 38, no. 6 (2020): 063203.

35. W. R. Flavell, A. G. Thomas, J. Hollingworth, et al., "Electronic Structure and Surface Reactivity of $La_{1-x}Sr_xCoO_3$," *Faraday Discussions* 114 (1999): 407–420.

36. "Surface Science Spectra," http://pubs.aip.org/avs/sss.

37. S. J. Freakley, J. Ruiz-Esquius, and D. J. Morgan, "The X-Ray Photoelectron Spectra of Ir, IrO_2 and $IrCl_3$ Revisited," *Surface and Interface Analysis* 49, no. 8 (2017): 794–799.

38. G. K. Wertheim and H. J. Guggenheim, "Conduction-Electron Screening in Metallic Oxides: IrO_2," *Physical Review B* 22, no. 10 (1980): 4680–4683.

39. H. Idriss, "On the Wrong Assignment of the XPS O1s Signal at 531–532 eV Attributed to Oxygen Vacancies in Photo- and Electro-Catalysts for Water Splitting and Other Materials Applications," *Surface Science* 712 (2021): 121894.

40. H. Idriss, "Oxygen Vacancies Role in Thermally Driven and Photon Driven Catalytic Reactions," *Chem Catalysis* 2, no. 7 (2022): 1549–1560.

41. T. J. Frankcombe and Y. Liu, "Interpretation of Oxygen 1s X-Ray Photoelectron Spectroscopy of ZnO," *Chemistry of Materials* 35 (2023): 5468–5474.

42. A. Posada-Borbón, N. Bosio, and H. Grönbeck, "On the Signatures of Oxygen Vacancies in O1s Core Level Shifts," *Surface Science* 705 (2021): 121761.

43. N. Bosio, A. Schaefer, and H. Grönbeck, "Can Oxygen Vacancies in Ceria Surfaces Be Measured by O1s Photoemission Spectroscopy?," *Journal of Physics: Condensed Matter* 34, no. 17 (2022): 174004.

44. T. Taniguchi, T. Watanabe, N. Sugiyama, et al., "Identifying Defects in Ceria-Based Nanocrystals by UV Resonance Raman Spectroscopy," *Journal of Physical Chemistry C* 113, no. 46 (2009): 19789–19793.

45. Y. Xu, F. Wang, X. Liu, et al., "Resolving a Decade-Long Question of Oxygen Defects in Raman Spectra of Ceria-Based Catalysts at Atomic Level," *Journal of Physical Chemistry C* 123, no. 31 (2019): 18889–18894.

46. L.-Q. Wang, D. R. Baer, M. H. Engelhard, and A. N. Shultz, "The Adsorption of Liquid and Vapor Water on TiO_2(110) Surfaces: The Role of Defects," *Surface Science* 344, no. 3 (1995): 237–250.

47. H. Idriss and M. A. Barteau, "Active Sites on Oxides: From Single Crystals to Catalysts," (2000) pp. 261–331.

48. H. Idriss and E. G. Seebauer, "Effect of Oxygen Electronic Polarisability on Catalytic Reactions Over Oxides," *Catalysis Letters* 66, no. 3 (2000): 139–145.

49. A. Walsh, A. A. Sokol, J. Buckeridge, D. O. Scanlon, and C. R. A. Catlow, "Oxidation States and Ionicity," *Nature Materials* 17, no. 11 (2018): 958–964.

50. P. S. Bagus, E. S. Ilton, and C. J. Nelin, "The Interpretation of XPS Spectra: Insights Into Materials Properties," *Surface Science Reports* 68, no. 2 (2013): 273–304.

51. P. S. Bagus, F. Illas, G. Pacchioni, and F. Parmigiani, "Mechanisms Responsible for Chemical Shifts of Core-Level Binding Energies and Their Relationship to Chemical Bonding," *Journal of Electron Spectroscopy and Related Phenomena* 100, no. 1–3 (1999): 215–236.

52. P. S. Bagus, C. J. Nelin, and C. R. Brundle, "Chemical Significance of X-Ray Photoelectron Spectroscopy Binding Energy Shifts: A Perspective," *Journal of Vacuum Science & Technology A* 41, no. 6 (2023): 068501.

53. P. M. Dietrich, S. Bahr, T. Yamamoto, M. Meyer, and A. Thissen, "Chemical Surface Analysis on Materials and Devices Under Functional Conditions—Environmental Photoelectron Spectroscopy as Non-Destructive Tool for Routine Characterization," *Journal of Electron Spectroscopy and Related Phenomena* 231 (2019): 118–126.

54. M. Kjærvik, P. M. Dietrich, A. Thissen, et al., "Application of Near-Ambient Pressure X-Ray Photoelectron Spectroscopy (NAP-XPS) in an In-Situ Analysis of the Stability of the Surface-Supported Metal-Organic Framework HKUST-1 in Water, Methanol and Pyridine Atmospheres," *Journal of Electron Spectroscopy and Related Phenomena* 247 (2021): 147042.

55. C. Byrne, K. M. Zahra, S. Dhaliwal, et al., "A Combined Laboratory and Synchrotron *In-Situ* Photoemission Study of the Rutile TiO_2 (110)/Water Interface," *Journal of Physics D: Applied Physics* 54, no. 19 (2021): 194001.

56. T. G. Avval, S. Chatterjee, G. T. Hodges, et al., "Oxygen Gas, O_2(g), by Near-Ambient Pressure XPS," *Surface Science Spectra* 26, no. 1 (2019): 014021.

57. T. G. Avval, S. Chatterjee, S. Bahr, et al., "Carbon Dioxide Gas, CO_2(g), by Near-Ambient Pressure XPS," *Surface Science Spectra* 26, no. 1 (2019): 014022.

58. I. P. Prosvirin, A. V. Bukhtiyarov, H. Bluhm, and V. I. Bukhtiyarov, "Application of Near Ambient Pressure Gas-Phase X-Ray Photoelectron Spectroscopy to the Investigation of Catalytic Properties of Copper in Methanol Oxidation," *Applied Surface Science* 363 (2016): 303–309.

59. L. Zhong, D. Chen, and S. Zafeiratos, "A Mini Review of *In Situ* Near-Ambient Pressure XPS Studies on Non-Noble, Late Transition Metal Catalysts," *Catalysis Science & Technology* 9, no. 15 (2019): 3851–3867.